Defect and Diffusion Forum Vol 363 (2015) pp 62-67

doi:10.4028/www.scientific.net/DDF.363.62

Lithium Diffusion in Li-rich and Li-poor Amorphous Lithium Niobate

Johanna Rahn[1,*], Benjamin Ruprecht[2], Paul Heitjans[2,3], Harald Schmidt[1,3]

[1]Technische Universität Clausthal, Institut für Metallurgie, AG Mikrokinetik, Clausthal-Zellerfeld, Germany

[2]Leibniz Universität Hannover, Institut für Physikalische Chemie und Elektrochemie, Germany

[3]ZFM - Zentrum für Festkörperchemie und Neue Materialien, Hannover, Germany

*johanna.rahn@tu-clausthal.de

Keywords: Amorphous lithium niobate, self-diffusion, isotope hetero-structures, secondary ion mass spectrometry

Abstract. The diffusion of lithium in amorphous lithium niobate layers is studied as a function of temperature between 293 and 423 K. About 800 nm thick amorphous $^{7}LiNbO_3$ layers were deposited on sapphire substrates by ion-beam sputtering. As a tracer source about 20 nm thin $^{6}LiNbO_3$ layers were sputtered on top. Isotope depth profile analysis is done by secondary ion mass spectrometry. Compared are amorphous samples which show a ratio of Li : Nb < 1 (Li-poor) and of Li : Nb > 1 (Li-rich) close to the stoichiometric composition of Li : Nb = 1 for crystalline $LiNbO_3$. The results reveal that the diffusivities of both types of samples obey the Arrhenius law with an activation enthalpy of 0.70 eV and 0.83 eV, respectively. The diffusivities of the sample containing a higher amount of Li are lower by a factor of about two to ten. This demonstrates that variation of the Li content in amorphous samples over the stability range of the crystalline $LiNbO_3$ phase has only a modest influence on diffusivities and activation enthalpies.

Introduction

Lithium niobate single crystals are technologically important synthetic oxides with extraordinary ferroelectric, piezoelectric, electro-optic and acoustic properties [1,2]. They are used as multifunctional materials, primarily in optics. The knowledge of lithium diffusivities at low temperatures is important to understand dark conductivity, thermal fixing of holograms, to avoid optical damage in wave guides, and for the creation, stability and dissociation of defect clusters. Lithium diffusion at low temperatures (below 800 K) was investigated by tracer methods with secondary ion mass spectrometry [3,4] or neutron reflectometry [5,6] and by conductivity measurements [7,8].

Amorphous lithium niobate films, however, are an interesting material for use as part of solid state lithium-ion batteries [9,10] due to its high chemical stability and increased ion conductivity [11] and diffusivity [12] compared to the crystalline state. In addition, lithium niobate thin films are interesting in surface sensitive applications. In the crystalline state, etching is very difficult, but amorphous films can be easily patterned by conventional photolithography and can be used as a precursor for crystalline film production [13]. Here, diffusion properties are interesting because they may govern microstructural re-arrangement processes.

The aim of the present paper is to investigate Li self-diffusion in ion-beam sputtered amorphous lithium niobate for Li-poor and Li-rich compositions close to the stoichiometric composition of Li : Nb = 1 in comparison.

Experimental

Tracer diffusion studies in Li containing solids have to be carried out with stable tracers because the classical radiotracer method cannot be used due to the fact that radioactive tracer isotopes with a half-life larger than some seconds do not exist. Lithium has two stable isotopes ^{6}Li (7.5 %) and ^{7}Li (92.5 %). For the diffusion studies, amorphous $^{7}LiNbO_3$ films (thickness: 800 nm) were prepared by ion-beam sputtering. ^{7}Li is preferred over ^{nat}Li in order to minimize the natural isotope background.

As substrates, 10 x 10 x 0.5 mm³ c-axis oriented polished sapphire single crystals from CrysTec (Berlin, Germany) were used. On top of the $^{7}LiNbO_3$ films tracer layers of $^{6}LiNbO_3$ (~ 20 nm) were deposited. This results in an isotope hetero-structure, where Li self-diffusion can be measured by pure isotope interdiffusion [14-17]. Ion-beam sputtering was done using a commercial set-up (IBC 681, Gatan) equipped with two penning ion sources. Deposition was done at 5 keV and at a current of about 200 µA in argon at an operation pressure of 5 x 10^{-5} mbar. The base pressure was better than
5 x 10^{-7} mbar. The sputter process was carried out at room temperature and no significant heating of the substrate took place. Sharp isotope interfaces can be produced. The structural state of $LiNbO_3$ was characterized by grazing incidence X-ray diffractometry on a Bruker D5000 diffractometer using CoK_α radiation.

Sputter targets were prepared by solid state syntheses. In an agate mortar coarse Nb_2O_5 (99.9985%, Alfa Aesar) was pestled to a fine powder and mixed with enriched $^{6}Li_2CO_3$ (96% ^{6}Li, Eurisotop) or $^{7}Li_2CO_3$ (99.9 % ^{7}Li, Alfa Aesar), respectively. After subsequent ball milling the powder mixture in a SPEX 8000M shaker mill, pellets of 2 cm in diameter were pressed and heated to 973 K with a rate of 2 K/min. The reaction step was followed by a sintering process at 1173 K for 12 h, which yielded polycrystalline dense targets. Two different types of amorphous lithium niobate films were sputtered for the diffusion experiments. For the first one (termed Li-poor) the molar ratio of oxide and carbonate used in the sputter target was chosen as 5:6, while for the second one (termed Li-rich) it was chosen as 1:3. These ratios were empirically determined, also in order to account for the loss of lithium during the sputtering process.

For the diffusion experiments the prepared samples were annealed in an argon atmosphere between 333 and 423 K using a commercial rapid annealing setup (AO 500, MBE, Germany). The annealing time was between 15 seconds and 2 minutes. At room temperature both types of materials show non-negligible ionic Li diffusion. The diffusivities at room temperature were determined by storing the samples simply for times up to about one day at ambient conditions and analyzing the isotope distribution subsequently at different storing times. Diffusivities at enhanced temperature were corrected by the room temperature diffusion effect as described in [12].

Secondary ion mass spectrometry (SIMS) investigations were carried out using a Cameca ims 3f/4f machine. Because of electrical charging during the measurements we used an O^- primary ion beam (15 keV, 30 nA). The sputtering area was of 250 x 250 µm². For analysis of the isotopes in a double focused mass spectrometer the signal resulting from an area of about 60 x 60 µm² in the center of the sputtering area is used in order to exclude crater edge effects.

The intensities of the $^{6}Li^+$ and $^{7}Li^+$ secondary ions were measured as a function of sputter time in depth profiling mode. Since the two Li isotopes are chemically identical (neglecting the small isotope effect), the intensity of the signals is converted into ^{6}Li atomic fractions *c(x,t)* according to

$$c(x,t) = \frac{I(^{6}\mathrm{Li})}{I(^{6}\mathrm{Li}) + I(^{7}\mathrm{Li})} \quad (1)$$

The depth of each measurement crater was quantified by a mechanical profilometer (Tencor, Alphastep) and used for depth calibration.

Results and Discussion

X-ray diffraction patterns of several hundred nanometer thick sputtered lithium niobate layers in the as-deposited state and after annealing at different temperatures were recorded for both types of samples under investigation. The results are given in Fig. 1. As obvious, the layers are X-ray amorphous after deposition. Annealing up to 623 K for 10 h showed (Fig. 1 (a)), that there still no crystallization occurs. Investigations on sputter layers annealed at higher temperatures between 673 and 923 K for 1 h show characteristic Bragg peaks. The dominating Bragg peaks can be attributed to the $LiNbO_3$ (space group R3c) phase for both type of films. For films with the Li-poor composition additional formation of the $LiNb_3O_8$ phase (space group $P2_1/c$) is observed (Fig. 1(a)).

Note that annealing at 773 K on the same type of sample gives no indication for impurity phases [12]. At a temperature of 823 K a decomposition of the $LiNbO_3$ phase into $LiNb_3O_8$ and Li_2O occurs during annealing. For films with Li-rich composition, the Li_3NbO_4 phase (space group I-43m) is additionally observed at 923 K (Fig. 1(b)). The phase fraction of these impurity phases is estimated to about five to ten percent and peaks corresponding to these phases are shown in Fig. 1 as grey shaded areas. The present XRD results show that both types of samples are amorphous after deposition with an approximate composition corresponding to $LiNbO_3$. However, analysis on samples annealed at 923 K indicate that the chemical composition of the two types of amorphous samples has to be located at the Li-poor and Li-rich border of the composition range of the crystalline compound $LiNbO_3$.

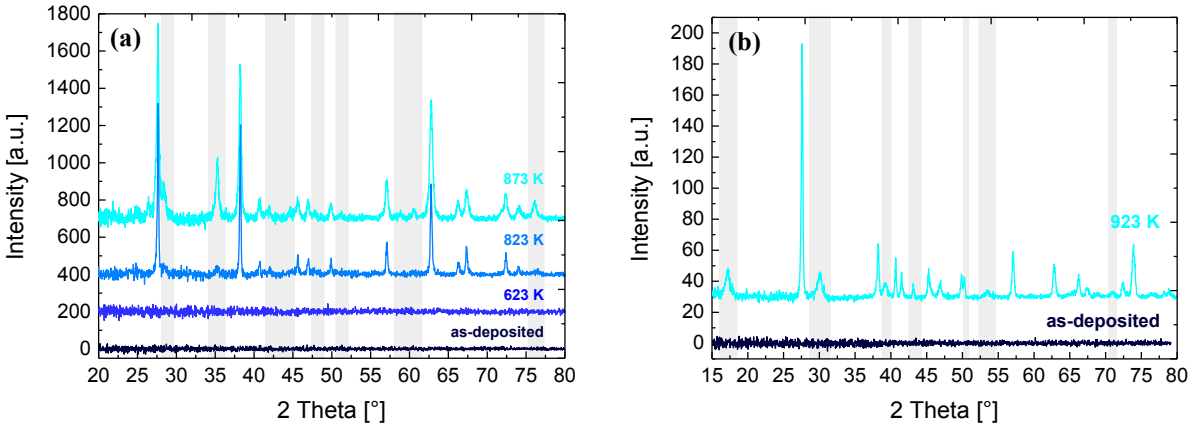

Figure 1 X-ray diffraction patterns of sputter layers after deposition and after annealing at elevated temperatures for 1 h for **(a)** Li-poor and **(b)** Li-rich lithium niobate compositions. For clarity, the patterns are shifted to higher intensity. The peaks marked by grey shaded areas correspond to the impurity phases $LiNb_3O_8$ (case (**a**)) and Li_3NbO_4 (case (**b**)), all other peaks correspond to $LiNbO_3$.

In Fig. 2 typical SIMS isotope depths profiles of an as-deposited and an annealed sample (20 s at 423 K) are shown. The penetration of ^6Li into the ^7Li enriched film by isotope diffusion is clearly seen. The experimentally determined depth profiles can be fitted by the following solution of Fick's second law for self-diffusion across an interface [18]

$$c(x,t) = c_\infty + \frac{(c_0 - c_\infty)}{2}\left[erf\left(\frac{h+x}{R}\right) + erf\left(\frac{h-x}{R}\right)\right] \tag{2}$$

where c_∞ is the relative isotope fraction of ^6Li in the amorphous $^7LiNbO_3$ layer and c_0 that in the $^6LiNbO_3$ tracer layer. The original thickness of the as-deposited tracer layer is denoted as h, which is 20 to 30 nm (sample dependent). The quantity R describes the broadening of the tracer profile and is used to determine the lithium self-diffusivity, D, which is calculated from the difference in R of the diffusion profile and of a starting profile, R_0, according to

$$D = \frac{\left(R^2 - R_0^2\right)}{4t} \tag{3}$$

where t is the annealing time. The quantities h and c_∞ are kept constant during the fitting procedure, while R and c_0 are free fit parameters

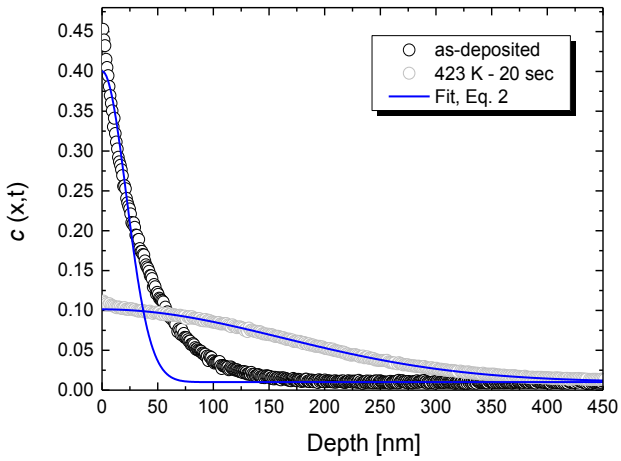

Figure 2 Atomic fraction of ^{6}Li as a function of depth measured by SIMS for an as-deposited sample and a sample annealed at 423 K for 20 s (Li-rich). Also shown are fits according to equation (2). The deviation of the fit from the experimental data at low ^{6}Li fractions is due to sputter induced forward mixing and does not significantly influence the determination of diffusivities. Note that an analysis based on the thin film solution of Ficks second law, instead of equation 2, gives the same diffusivities within error limits.

The diffusivities at room temperature are shown in Fig. 3 as a function of storage time. As obvious, the data are identical within error limits and a possible annealing time dependence of diffusivities could be excluded. The lacking time dependence of diffusivities illustrates that diffusion in these amorphous materials takes place in a relatively rigid matrix, which is formed by the Nb-O network. This network (bonds, bond angles, atomic distances) and the resulting activation barriers are not significantly modified during annealing at these low temperatures. Li is the species with the highest ionic mobility that migrates through the Nb-O network, governed by an effective activation enthalpy resulting from an averaging over several non-equal jumps in the amorphous matrix. One can think of some kind of "structural vacancies" to be present, where the vacancy concentration is fixed by a frozen-in defect structure formed during sputter deposition.

All measured diffusivities are plotted in Fig. 4 as a function of reciprocal temperature. The data for each type of material obey the Arrhenius law

$$D = D_0 exp\left(\frac{-\Delta H}{k_B T}\right) \tag{4}$$

where k_B is the Boltzmann constant and T is the temperature. We get an activation enthalpy of ΔH = (0.70 ± 0.03) eV for the Li-poor sample (as already published in [12]) and ΔH = (0.83 ± 0.03) eV for the Li-rich sample in the temperature range between 293 and 423 K. The corresponding values for the pre-exponential factors are D_0 = 5.0 x 10^{-7} m²/s (error: ln D_0/m²/s = ± 1.2) and D_0 = 1.2 x 10^{-5} m²/s (error: ln D_0/m²/s = ± 0.9), respectively.

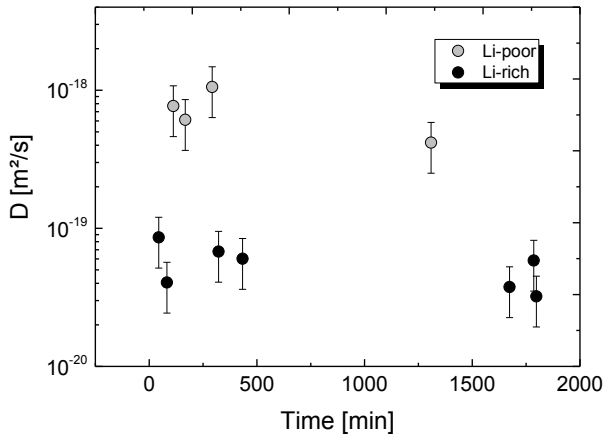

Figure 3 Lithium diffusivities, *D*, for various storage times in amorphous lithium niobate at room temperature for Li-rich (293 K) and Li-poor samples (297 K).

As obvious from Fig. 4, the diffusivities of the sample containing a higher amount of Li is lower by a factor of about two to ten. This shift results from a combined increase of both the activation enthalpy and the pre-exponential factor of the Li-rich sample due to some kind of compensation effect. The increase of the two separate quantities results in a small modification of the diffusivity only. A similar effect was found in electrical conductivity measurements at higher temperatures above 800 K on near stoichiometric and congruent lithium niobate single crystals [19]. If the validity of the Nernst-Einstein equation is assumed and the concentration of the Li ions as charge carriers is assumed to be approximately constant, this can also be traced back to be the consequence of a variation of diffusivities. The observed difference in diffusivities of Li-rich and Li-poor amorphous samples indicates that the rigid Nb-O network, where Li is diffusing in, is not much different for both type of samples. But the slightly higher amount of Li in the Li-rich sample seems to block the Li mobility and slows down the diffusion of Li through the network. The higher the annealing temperatures the less this effect has influence on the diffusivities. As also visible in Fig. 4, the diffusivities of the $LiNbO_3$ single crystals are lower by several orders of magnitude if compared at the same temperature, due to a more dense packed structure (see also [12]).

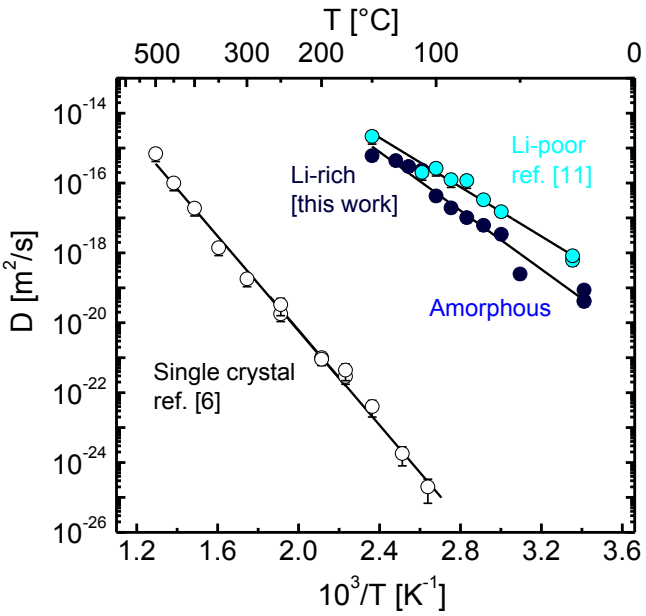

Figure 4 Lithium diffusivities, *D*, in amorphous lithium niobate as a function of reciprocal temperature in comparison to the diffusivities of a lithium niobate single crystal [3,6].

Summary

Tracer diffusion experiments with isotope hetero-structures and SIMS were carried out in order to investigate lithium self-diffusion in amorphous lithium niobate layers with different Li contents (lower/higher), but close to the stoichiometric composition of the crystalline $LiNbO_3$ phase. We determined diffusivities in the temperature range between 293 and 423 K. An Arrhenius behavior is found with an activation enthalpy of 0.70 eV and 0.83 eV, respectively. The diffusivities of the sample containing a higher amount of Li are lower by a maximum factor of about ten, indicating a modest influence of Li content on diffusivities.

Acknowledgements

Financial support from the Deutsche Forschungsgemeinschaft (projects: Schm 1569/18 and He 1574/13) in the framework of the Research Unit FOR 1277 (‘molife’) is gratefully acknowledged. We thank L. Dörrer for assistance in SIMS analysis and G. Borchardt for the permission to use his SIMS equipment.

References

[1] T. Volk, M. Wöhlecke, Lithium Niobate, Springer, Berlin, 2010.

[2] K. K. Wong, Properties of Lithium Niobate, Inspec, London, 2002.

[3] J. Rahn, E. Hüger, L. Dörrer, B. Ruprecht, P. Heitjans, H. Schmidt, Phys. Chem. Chem. Phys. 14 (2012) 2427.

[4] J. Rahn, L. Dörrer, B. Ruprecht, P, Heitjans, H. Schmidt, Defect-Diffus. Forum 333 (2013) 33.

[5] E. Hüger, J. Rahn, J. Stahn, T. Geue, H. Schmidt, Phys. Rev. B 85 (2012) 214102.

[6] E. Hüger, J. Rahn, J. Stahn, T. Geue, P. Heitjans, H. Schmidt, Phys. Chem. Chem. Phys. 16 (2014) 8670.

[7] M. Masoud, P. Heitjans, Defect-Diffus. Forum 237-240 (2005) 1016.

[8] B. Ruprecht, J. Rahn, H. Schmidt, P. Heitjans, Z. Phys. Chem. 226 (2012) 431.

[9] N. Kamaya et al., Nat. Mater. 10 (2011) 682.

[10] M. Ogawa, R. Kanda, K. Yoshida, T. Uemura, K. Harada, J. Power Sources 205 (2012) 487.

[11] P. Heitjans, M. Masoud, A. Feldhoff, M. Wilkening, Faraday Discuss. 134 (2007) 67.

[12] J. Rahn, E. Hüger, L. Dörrer, B. Ruprecht, P. Heitjans, H. Schmidt, Z. Phys. Chem. 226 (2012) 439.

[13] V. Joshkin, K. Dovidenko, S. Oktyabrsky, D. Saulys, T. Kuech, L. McCaughan, J. Cryst. Growth, 259 (2003) 273.

[14] H. Schmidt et al., J. Appl. Phys. 93 (2003) 907.

[15] H. Schmidt, U. Geckle, M. Bruns, Phys. Rev. B. 74 (2006) 045203.

[16] E. Hüger, U. Tietze, D. Lott, H. Bracht, E. E. Haller, D. Bougeard, H. Schmidt, Appl. Phys. Lett. 93 (2008) 162104.

[17] H. A. Bracht, H. H. Silvestri, E. E. Haller, Solid State Commun. 133 (2005) 727.

[18] J. Crank, The Mathematics of Diffusion, Oxford University Press, Oxford, 1975.

[19] A. Weidenfelder, J. Shi, P. Fielitz, G. Borchardt, K. D. Becker, H. Fritze, Solid State Ionics 225 (2012) 26.